OPTIMIZED CONTROL OF SLAG CHEMISTRY FOR THE ELECTROSLAG REMELTING OF LARGE SIZE INGOTS.

J. Reitz[1], M. Maurischat[2], B. Friedrich[1]

[1] IME Process Metallurgy and Metals Recycling, RWTH-Aachen University, Intzestr. 3, D-52072 Aachen

[2] Saarschmiede GmbH, Bismarckstraße 57-59, D-66333 Völklingen

1 Summary

Assessing electroslag remelting of large size ingots from special steels, the major parameter for quality of the metal ingot is axial chemical homogeneity. The investigations presented in this paper show, that process control for the feeding of deoxidants cannot purely rely on thermochemical calculations, because slow kinetic effects delay the progress towards chemical equilibrium, leading to unexpected variations in slag- and metal composition. A production orientated mathematical model was developed to predict the evolution of slag chemistry based on analysis of sampling data from previous runs. To adjust the model with the necessary parameters, 17 industrial melts were evaluated. The presented work is the basis for development of an expert system that should ensure stable control of slag chemistry in the near future.

2 Introduction

In the electroslag remelting (ESR) of 175 t ingots from chromium steels for heavy forging applications, typical melting times are in the order four days. Among other criteria the quality of the final product is measured by the chemical homogeneity of the metal block, mainly in direction of it's main axis. As a major characteristic in ESR, only a partial volume of the metal is molten at a time and back-mixing is limited to the melt pool which is in contact with the slag. The composition of the metal pool is not only depending on the alloy fed from the electrodes, but also to the evolution of slag chemistry during this melting process, which typically takes place at atmospheric conditions at such a large scale. To ensure chemical homogeneity of block, it is necessary to carefully control the activities of the slag components.

From a thermochemical perspective the slagging reaction i.e. the transfer of an element from the metal phase to the slag, of important alloying elements like Cr, Mn or B depends on the oxygen potential of the slag, reversely depending on its composition which is continuously changing during the melt by uptake of oxides if no countermeasures are taken. This field is a matter of interest since the beginning of ESR, describe e.g. by Biele [1] and Mitchell [2]. To avoid the loss of alloying elements below a certain level it is industrial practice nowadays to feed various master alloys directly into the slag, which are serving as deoxidation agents. At high content of strongly reducing metals such slags are sometimes referred to as "reactive slags" throughout the literature. From a process control perspective it is crucial to feed the correct amount of deoxidants adjusting the appropriate alloying level in the final product [3].

The investigations presented in this paper show, that process control for the feeding of deoxidation agents in large scale ESR furnaces cannot purely rely on thermochemical calculations because slow kinetic effects delay the state of chemical equilibrium, leading to unexpected variations in slag- and metal composition. Furthermore there is no industrial method at present to measure the oxygen potential of the slag correctly which could offer direct control of the process. Because of the complex nature of the occurring kinetic effects, a mathematical model was developed to predict the evolution of slag chemistry based on sampling data from previous production runs. This model will serve as a basis for a future expert system to ensure stable control of slag chemistry by accurate feeding of deoxidants.

3 Methods, techniques, materials

3.1 Description of the system

This investigation is based on the evaluation of data from industrial ESR melts. The typical composition of the steel related to this work is given in Table 1.

Table 1: Typical composition of examined steels

	Cr	Mo	W	Ni	Mn	V	Nb	Si	Al
w%	10	1	1	0,7	0,4	0,2	0,35	0,081	0,08

Table 2: Changing levels of oxide components in the ESR slag. Balance CaO and CaF_2

In w%	SiO_2	FeO	MnO	Al_2O_3	Cr_2O_3	TiO_2
Min	2,27	0,1	0,16	23,3	0,31	0,05
Max	3,87	0,14	0,33	34,7	0,46	0,12
Avg	2,92	0,12	0,25	28,51	0,38	0,09

At the start of the process, two different standardized slags are blended to adjust a well-proven composition. The slag composition changes during the melt, due to oxygen pickup and fluorine evaporation. Typical average analyses and the span are given in Table 2 with the balance components being fluorspar and lime as usual in ESR practice.

3.2 Thermochemistry

Slag systems used for ESR are molten oxide-fluoride systems, with the overall viewpoint in literature, that anions like O^{2-} and F^- are building up an electrically neutral liquid network with various cations, Si^{4+}, $Fe^{3+/2+(6+)}$, $Mn^{2+\,(7+,6+,4+,3+)}$, Al^{3+}, $Cr^{3+(2+)}$, $Ti^{4+,(3+)}$, $Ca^{2+,(1+)}$ (less common oxidation numbers given in brackets). In addition to this simple model various polymerisation and complex reactions that go beyond the scope of this work have been discussed [4]. A major feature of our understanding of metallurgical slags is, that the cations of transition metals can commonly assume several oxidation states e.g. Fe^{2+} vs. Fe^{3+}, accounting for a series of slag phenomena from electrical conductivity to chemical activity.

Imagining a slag dissolves metallic materials fed into the system, essentially, the first possibility is atomic dissolution in the ionic liquid up to a certain degree. Also a disproportioning mechanism was discussed [5]. Furthermore it can be imagined, that comparatively reducing (ignoble) metals in contact with oxides of more noble metals in a slag react by being converted into cations, while transferring electrons to the slag. As the slag must remain electrically neutral, such a reaction can only be imagined by transfer of other cations into transition states by electron exchange, e.g.

$$Ca + 2\,Fe^{3+} <=> Ca^{2+} + 2\,Fe^{2+} \qquad (1)$$

At the same time, the slag is in contact with an oxidizing environment, e.g. the atmosphere at the slag-gas interface. Oxygen is eventually dissolved in atomic form, and substantial dissociation can take place, depending on the type and concentration of cations dissolved in the slag [6][7].

$$O^{2-} + O_{,dissolved} <=> 2\,O^- \qquad (2)$$

If the slag is subjected to a feed of reducing metals and oxygen at the same time, it can be argued, that semi-stable cations and anions would equal out within the slag giving an equilibrium reaction between the two.

$$O^- + Fe^{2+} <=> O^{2-} + Fe^{3+} \qquad (3)$$

Independent of the actual mechanism, it can be concluded, that reducing metals can render the slag into a state of lower oxygen potential, represented by a high level of either cations or anions in their semi-stable oxidation state. Vice-versa, intensive contact with oxygen brings the slag to a state of high oxygen potential with low concentration of reducing ions.

Such a slag, in contact with a metallic melt pool should be able to either oxidize components of the metallic melt (e.g. Mn) and form cations incorporated into the slag or vice-versa, reduce cations and dissolve the component in the metal pool as indicated above.

$$Mn_{met} + 2O^- <=> Mn^{2+} + 2O^{2-} \qquad (4)$$

$$Mn^{2+} + 2\,Fe^{2+} <=> Mn_{met} + 2\,Fe^{3+} \qquad (5)$$

The preferred direction of the equation is a function of the oxygen potential, given by either the activity of oxidizing anions or the activity of reducing cations (a_i) and the activity of Mn in the melt pool, as well as the equilibrium constant K , i.e. ΔG for the respective metals.

$$K' = \frac{a\left(Mn^{2+}\right)_{slag}}{a(Mn)_{met} \cdot a\left(O^-\right)_{slag}} \qquad (6)$$

$$K'' = \frac{a(Mn)_{met} \cdot a\left(Fe^{3+}\right)_{slag}}{a\left(Mn^{2+}\right)_{slag} \cdot a\left(Fe^{2+}\right)_{slag}} \qquad (7)$$

For the equilibrium state, a distribution coefficient DC between the metal in the slag and the respective oxide in the slag can be defined based on their weight based concentration in the respective phase. It should be expected, that in equilibrium conditions this distribution coefficient is a function of the above oxygen potential or the ratio of e.g. the polyvalent Fe-ions respectively.

$$DC_{Mn} = \frac{w(MnO)_{slag}}{w(Mn)_{metal}} = f\left(a(O)_{slag}, \frac{a\left(Fe^{3+}\right)_{slag}}{a\left(Fe^{2+}\right)_{slag}} \right) \qquad (8)$$

If several elements are involved in the system of the metal pool and the slag it can be understood, that this interaction of oxidation and reduction is relatively complex for thermochemical description. Although interaction parameters for this kind of systems are available nowadays and the thermochemical description by ΔG-minimizing software like FactSage™ is quite accessible it was chosen to approach the present problem by more statistical methods because of the kinetic effects observed.

3.3 Kinetic considerations

In industrial ESR practice the slag equilibrium is continuously subjected to mass-exchange over the system boundaries sketched in Figure 1. While thermal conduction of the system occurs in all directions, with the major flow across the crucible walls [8], reactive mass-flow is limited to the slag-gas-interface and the slag metal-interface. Apart from the melt flow from the electrodes to the pool, a second major mass transfer into the slag occurs through the feeding of material, e.g. granules directly onto the slag surface, which will be absorbed by the slag by stirring and/or solution.

Gas-metal interfaces occur between the liquid downside of the electrode and the slag, the droplet surface, while travelling through the slag and the surface of the melt pool below the slag. A comprehensive summary of the occurring phenomena has been published by Hoyle [9]. Given the fact that residence times of the droplets are relatively short, while surface is comparatively small and the liquid electrode tip is continuously renewing, while being small in volume itself, the most significant surface for slag metal reactions is the interface to the molten pool.

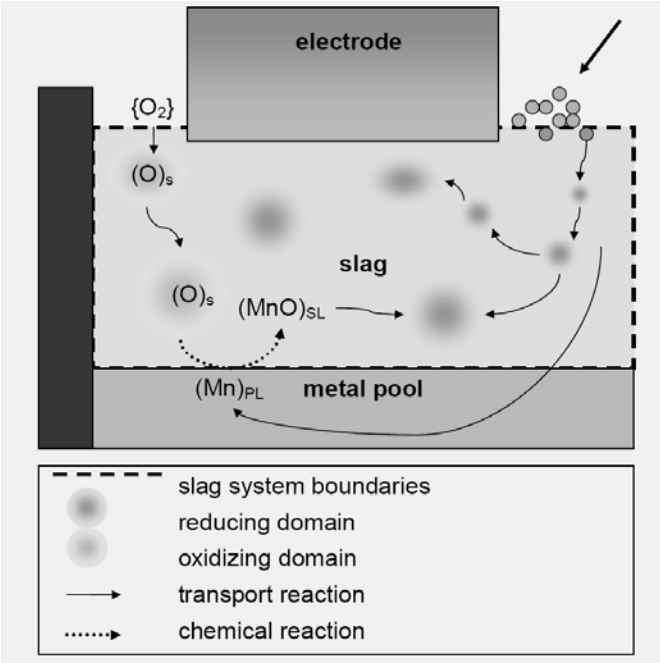

Figure 1: Simplified representation of the slag-metal system with feeding of solid desoxidation agent and reducing/oxidizing domains

It can be imagined, that a solid particle dropped onto the slag, heats up after contact, is eventually molten and drops below the slag surface by either/or convection or density difference. In case of a metallic particle, the described metal-slag reactions might occur. Depending on the stirring speed of the melt and surface reactions, this reaction will generate a moving, locally defined yet quickly expanding domain in the slag with lower oxygen activity.

The same holds for the pick-up of oxygen through the gas-slag interface. The oxidation of the electrode right above the melt and the solution of the respective scale represents another possibility for oxygen pick-up. Analogue to the reducing agents a moving and expanding domain of increased oxygen activity can be imagined.

Considering now, that oxidation of components from the metal will take place on the downside of the slag, namely at the metal pool, in can be easily understood, that significant transport of the oxidizing domains to the pool is necessary, while reduction of cations, eventually forming metallic droplets, might be directly possible within the slag or at the pool respectively.

For the present case, a fairly large slag-system is considered, with a slag bath diameter of 2300 mm. It can be imagined that transport-reactions are slower than in smaller ESR furnaces when stirring speeds are comparable and that the corresponding phenomena are significant. This goes in hand with the qualitative observation, that there is a measureable delay between the feeding of deoxidation agents and the corresponding effect on the slag-metal reactions.

It would go beyond the focus of this paper to derive an exact representation of all chemical and transport reactions involved in the system, apart from the fact that not much is known on the exact fluid flow in the furnace. Additional effects, like the obliteration of oxidizing and reducing zones during transport in the bulk of the slag would have to be taken into account, as well as diffusion effects in the boundary layers, eventually involving description of turbulent flow. Thus it was decided in the present work to chose an empirical approach in order to describe the overall kinetic effects of the system on the slag chemistry, based on a simple model and the evaluation of industrial melting data.

3.4 Selection of indicators

For the present observation of slag-metal kinetics and subsequent usage as a process control indicator several chemical elements could be chosen for observation. To minimize the sensitivity of the model for analytical failure, a ranking was carried out, to identify two elements which give the most reliable indication on the status of the slag, according to the following criteria:

- The component should be accessible to analysis in metal and slag samples in terms of concentration and analytical methods. (For this reason the elements Mo, W, and Ni were omitted the concentration of their oxides was not determined in the slag)
- Reaction of the metallic component on changes in deoxidizing agent feed should be as significant as possible.
- Because the analysis carried out observes the answer of the slag system to a change in deoxidizing agent, the elements chosen for observation should not be present in the deoxidizing agent itself.
- The element should not be Fe as the majority component of the metal.

3.5 Mass balance

For the elements selected, a differential mass balance was established by selecting the slag-gas and slag-metal-interfaces at the system boundaries. For a chosen element X, the law of mass conservation yields:

$$\frac{dm_{X,EL}}{dt} - \frac{dm_{X,SL}}{dt} - \frac{dm_{X,BL}}{dt} = \frac{dm_{X,PL}}{dt} \quad (9)$$

with the subscripts EL indicating the electrode, SL the slag phase, BL the solidified block and PL the metal pool. The mass of element X in phase Y is correlated to it's concentration and the mass of the phase:

$$m_{X,Y} = m_Y \cdot w_{X,Y} \quad (10)$$

Thus every change in mass over time has to be described as:

$$\frac{dm_{X,Y}}{dt} = \frac{dm_Y}{dt} \cdot w_{X,Y} + \frac{dw_{X,Y}}{dt} \cdot m_Y \quad (11)$$

For simplification the following assumptions are made: for large periods in time, the concentration $w_{X,EL}$ in the electrode is constant, the concentration $w_{X,BL}$ in the block is equal to the concentration in the melt pool $w_{X,PL}$, the total mass of the melt pool m_{PL} is constant over time and because of that the mass change of the electrode is equal to the mass change of the block (mass constancy), given by the melt rate MR. For the slag phase no simplifications can be made, because the total mass of slag and its composition are changing over time. With the given simplification, equation (9) can be transformed into the differential equation (12)

$$\frac{dm_{X,SL}}{dt} = -\frac{dw_{X,PL}}{dt}(m_{BL} + m_{PL}) - w_{X,PL} \cdot MR + w_{X,El} \cdot MR \quad (12)$$

It can be seen, that the change of a component in the slag is lately dependent on the transport of this element across the interface between the melt-pool and the slag and the transfer from the electrode, given by the electrode concentration. Thus, in a first approach, the database analysed features the concentration of the chosen element X in the melt pool, the slag and the electrode and the behaviour in all three phases was observed over time.

3.6 Rate of slagging

As a measure for the slagging rate, two indicators have been observed in this work. In a simple approach the concentration of the respective oxide $w_{X,SL}$ in the slag was plotted over time (see Figure 4). With the thermochemical principles of equilibrium in mind, a second indicator f for the speed of slagging was introduced as the ratio of the concentration of metal X in the pool with the concentration in the electrode presently molten (during the melting operation regular electrode changes occur, sometime involving electrodes from different batches with slightly varying concentrations)

$$f = \frac{w_{X,PL}}{w_{X,EL}} \quad (13)$$

In cases were no slagging occurs, f would approach unity with equal concentrations in electrode and pool. For significant slagging, the concentration in the pool would be lower than the one in the electrode and thus $f < 1$, while for weak slagging $f > 1$ would hold. Both indicators have been compared and one was chosen as a basis for the model according to the results.

3.7 Effectiveness of deoxidants

In the present analysis two different alloys A and B are fed to the system for desoxidation. Both alloys contain the ignoble metals M1 and M2 suitable for desoxidation of the metal, yet A and B show different concentrations of M1 and M2. In industrial practice, both alloys are fed to the system in arbitrary ratios and first observations have shown, that the correlation of slag behaviour to only one of the two components is nearly impossible, thus an aggregated value on the intensity of deoxidation had to be found and a simple semi-thermochemical approach was applied:

For both M1 and M2 their oxidation reaction (14) is driven by their Gibbs free energy ΔG^0. Because the density of M1 and M2 differs significantly and because the feeding of slag components is measured in grams per minute, those values were determined in J/g based on data from the FACT55 database supplied with the FactSage™ software.

$$X\ M(i) + y/2\ O <=> M(i)_xO_Y \quad \Delta G^0 < 0 \quad (14)$$

ΔG^0_{M1} = -5186,3 J/g, ΔG^0_{M2} = -7844,2 J/g at 1600°C

For every reducing agent A and B, the relative "intensity" of reduction was determined by a weighed average G^0_{av} in J / g. To have a common index, the level of desoxidation charging ID was determined according to equation (15), with m_I as the amount of desoxidation agent A and B respectively, which are fed to the process in intervals of Δt.

$$ID = \left(m_A \cdot G_{av,A} + m_B \cdot G_{av,B}\right) / \Delta t \ \text{ in J / g} \cdot \text{s} \quad (15)$$

3.8 Data collection

During the industrial melting operation, samples of slag and metal were taken in regular time intervals and recorded in MS ACCESS™ data sheets. Data on process control, like melt rates, power supply and charging of deoxidants were recorded in a separate database (see Figure 2). At the present stage, 120 sets of data from 11 industrial melts have been selected by defined conditions. From a larger database of available operation data only those sets were included via queries, that feature an analysis of the slag and the metal, a correct record of the sampling time, an analysis of the electrodes being remelt at that time, a measurement of slag temperature and information on the present charging rate for deoxidants A and B.

3.9 Building of a model

For every melt taken into account, chemical data was available on average at ten different melting times. In parallel to that, a second database features an entry every time the rate of deoxidants was changed. From the available data, several values were calculated, e.g. the overall intensity of the desoxidation agents (according to equation (15) or a common baseline time for comparison of all events.

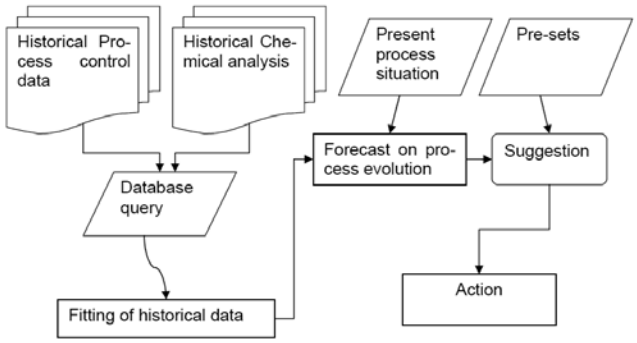

Figure 2: Workflow of the proposed system

In a second step an analysis was carried out to identify two relevant melts with high and low fluctuation of oxide concentration. For these melts, the evolution of slag chemistry and the changes in desoxidation feeding were plotted over time to view tendencies in melting behaviour (see Figure 3, numbers normalized to protect proprietary information of the industrial partner).

For the present approach, the slag is regarded as a black-box system. A change in the feed of desoxidation agents represents an impulse to the system in the sense of a Heaviside function, while the following slag samples represent the response of the system to that change.

As displayed in Figure 3, a change in deoxidation feeding is followed by a certain time of stationary feed. In that manner, every melt was “sliced” into sections between two changes in desoxidation feeding. In every section, a local time variable t_{local} equals 0 at the moment of deoxidation change.

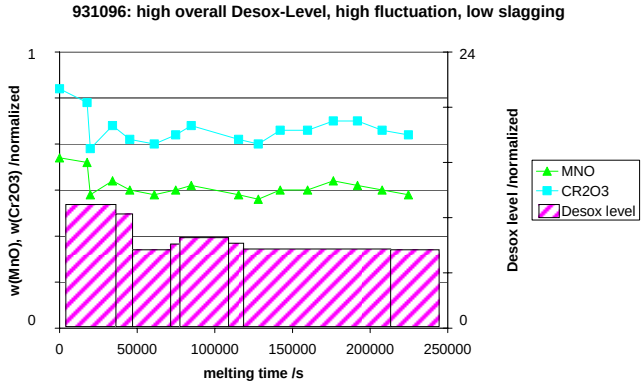

Figure 3: Development of slag chemistry and desoxidation level during melting.

For every section, it was assumed, that the evolution of oxide content after a change in desoxidation feeding can be fitted by the least squares method with a parabolic function according to equation (16), taking into account the last analysis before the deoxidation change (negative t_{local}), plus the following two analytic values.

$$c_{MnO}(t) = b \cdot m^t \qquad (16)$$

This was repeated for the whole set of melting data, giving a set of fitting values m and b. While b represents essentially the oxide concentration at the moment of desoxidation change $t_{local} = 0$, it is mainly dependent on the final concentration of the previous “slice”. In contrast to that, the parameter m should essentially be a function of the desoxidation intensity with $m < 1$ (negative slope) for very high desoxidation level and $m > 1$ (positive slope) for less feeding of desoxidation agents.

Thus m was described as a function of ID. Again a parabolic fit was chosen to define as m function of ID with the parameters m’ and b’. The combination of the derived values yields a simple model for the local prediction of the development of slag oxide level based on the present ID and the last chemical analysis at a desired time t.

$$c_{MnO}(t+\Delta t) = b \cdot \left(b' \cdot m'^{ID}\right)^{t+\Delta t} \qquad (17)$$

$$ID_f = \frac{\lg\left(SR \cdot \Delta t + c(MnO)_{t_0}\right) - \lg\left(c(MnO)_{t_0}\right) + \lg m_{t_0} - t \cdot \lg(b')}{t \cdot \lg(m')} \qquad (18)$$

In a first approach, this model was used to draw a predictive function based on the two selected melts, to compare the accuracy of the results. Furthermore, above equation was inverted into equation (18) to yield a future for ID, ID_f as a result of a slagging rate SR.

Based on the last chemical analysis and the present level of desoxidation feeding, it is now possible to predict the evolution of oxide level, compare with a wanted slagging rate and receive a prediction of what ID should be adjusted to, in order reach to that level.

4 Results

4.1 Stable conditions

On the examined melts the slag temperature was 1609°C on average, with a standard deviation of only 0,9%, thus changes of the equilibrium constants K' and K'', known to show the usual Arrhenius dependency on temperature, were considered to be insignificant for the evaluation of slag chemistry. The same holds for the atmosphere above the slag which was controlled by a constant stream of dried, compressed air as well as for the melt rates of the electrodes, which show a standard deviation of 15% within the same melt (due to a ramp-up after the start phase), but only a deviation of 1% when different melts are compared.

4.2 Selection of indicators

Six industrial melts have been observed in a first approach to find the most desoxidation sensitive elements in the slag. For every slag component the fluctuation in concentration over the whole melting time was expressed as the relative span RS.

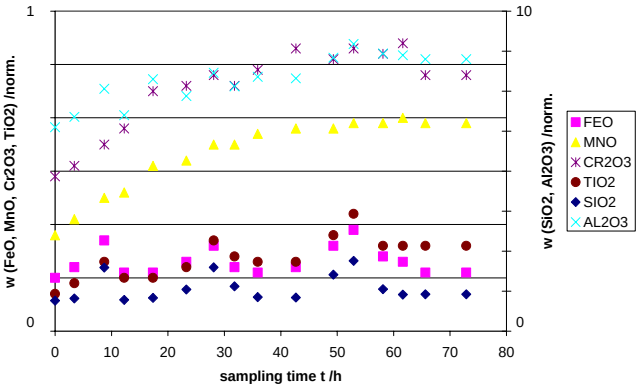

Figure 4: Typical evolution of oxide content

Unfortunately RS features large values for both elements that show large fluctuation during the melt as well as such elements that show large overall enrichment.

It can be seen visually from the plot of slag chemistry over time in Figure 4, that for Mn and Cr the level of their oxides is increasing over the melting time in addition to their reaction on the desoxidation agent. To gain a more accurate picture on the actual sensitivity on the level of desoxidation, the increase of the different oxide concentrations was fitted by a linear least squares approach, giving a slope m. As a second indicator for evaluation CF = 1-m was chosen, so that oxides which are fluctuating in concentration but are at the same time not significantly enriching in the slag would gain values approaching 1, while elements which are significantly enriching are receiving values < 1.

On this basis a final ranking could be established attributing higher ranks to elements which show a high relative span RS and are the same time relatively constant in their concentration over time, giving a high CF value. The elements of interest were ranked as follows:

CF(Ti) > CF(Mn) > CF(Cr) > CF(Si)

Considering the fact that in some of the analysed melts, Ti concentration is in the range of only 0,001% (10 ppm) it is highly probable that fluctuations in it's concentration can be attributed to analytical deviations. Thus Mn (~1% in metal phase, ~0,25% oxide in slag) and Cr (~10% in metal phase, ~0,4% in slag) were chosen to be in the main focus for building up the model. It can be observed, that the content of Cr_2O_3 and MnO in the slag behave synchronous suggestion that their reaction to the desoxidation agents is similar yielding a better accuracy for a model based on both indicators.

4.3 Thermochemical equilibrium

In a first approach, the concentration of Cr_2O_3 in all slag samples was plotted vs. the concentration of Cr in the melt pool. Based on the theoretical approach given above for thermochemical equilibrium, a clear dependency of the oxide content of the slag could be expected. It can be seen from Figure 5, that the process never seems to be in thermochemical equilibrium, with oxide contents being largely independent of the actual Cr concentration in the melt.

It was thus expected, that the concentration of the respective oxides in the slag would show a strong dependency on the level of desoxidation agents being charged.

Figure 6 shows that for such an overall dependency of the oxide level on the charging of deoxidants, the overall tendency is correct, yet shows a very weak correlation.

As a result it was clearly visible, that a simple thermochemical observation would not be sufficient to analyse and predict the behaviour of the slag due to time dependent deviation from thermochemical equilibrium; a more time-localized approach is necessary.

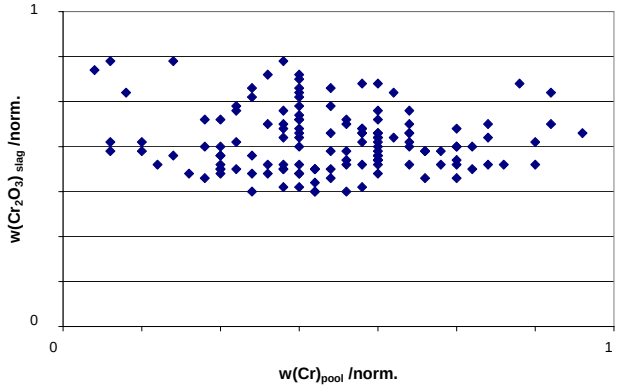

Figure 5: Concentration of Cr_2O_3 in the slag vs. concentration Cr in the melt shows no clear thermochemical behaviour

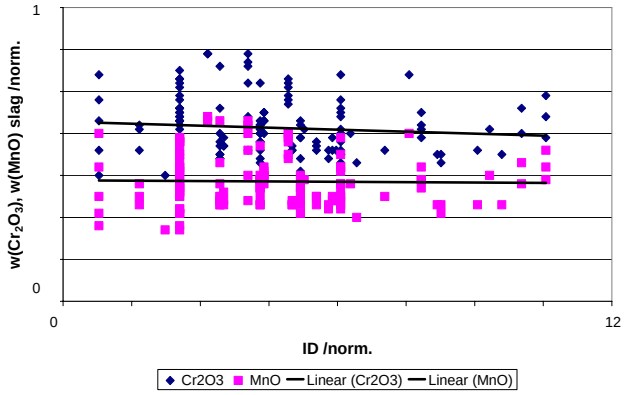

Figure 6: Dependency of oxide level on ID, overview of all melting data

4.4 Improvement of the model through averaging and introduction of slagging rate

For all the melts mentioned above the average intensity of desoxidation (ID) was determined, as well as the average concentration of MnO and the average value for the ratio f between Mn content in the melt pool and the electrode respectively. Both indicators have been plotted against the average ID and the expected tendency was clearly observed in the two cases (compare Figure 7): the higher ID, the lower the overall rate of slagging. Observing the concentration of MnO gives a better correlation (R^2=0,6) than the quotient f, i.e. w(MnO) was preferred for the next evaluation steps.

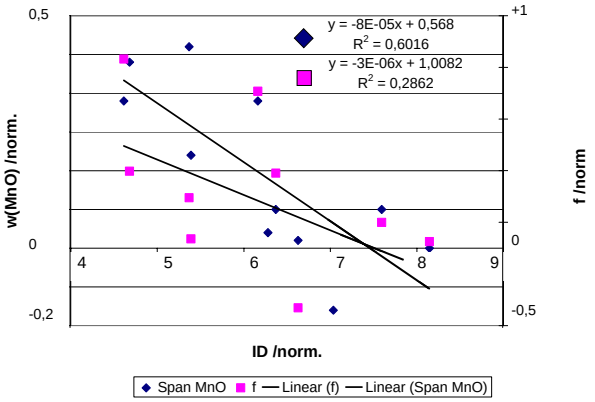

Figure 7: Dependency of average oxide concentration and slagging rate indicator f on the average ID.

According to the methods explained in 3.9, equation (17) was applied to the local "slices" and both MnO and Cr_2O_3 were plotted against ID for all melt slices. As can be seen from Figure 8, the expected tendency can be observed when applying a linear fit to values from one single melt. The general dependency m = f(ID) was derived by a parabolic fit and plotted for comparison (dashed line). As both m' and b' values derived are close to unity, the dependency appears close to linear on the graph. The same plot was repeated for Cr_2O_3 yielding a similar, behaviour but even more linear fit.

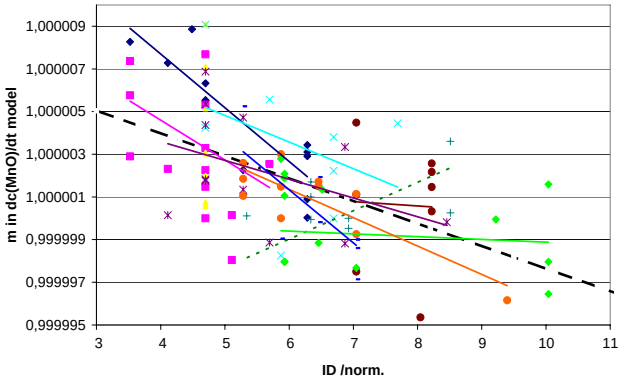

Figure 8: Local fitting parameter m as a function of ID (data for MnO)

4.5 Application of the model

The fitting values derived above were fed back into the model eq. (17) to serve as a forecast function for the two selected melts. For demonstration a forecasting time of 10.000 s was selected for every melt section and plotted together with the sampled evolution of the slag chemistry. Reasonable agreement can be seen in Figure 9 a, b, indicated by interconnected data.

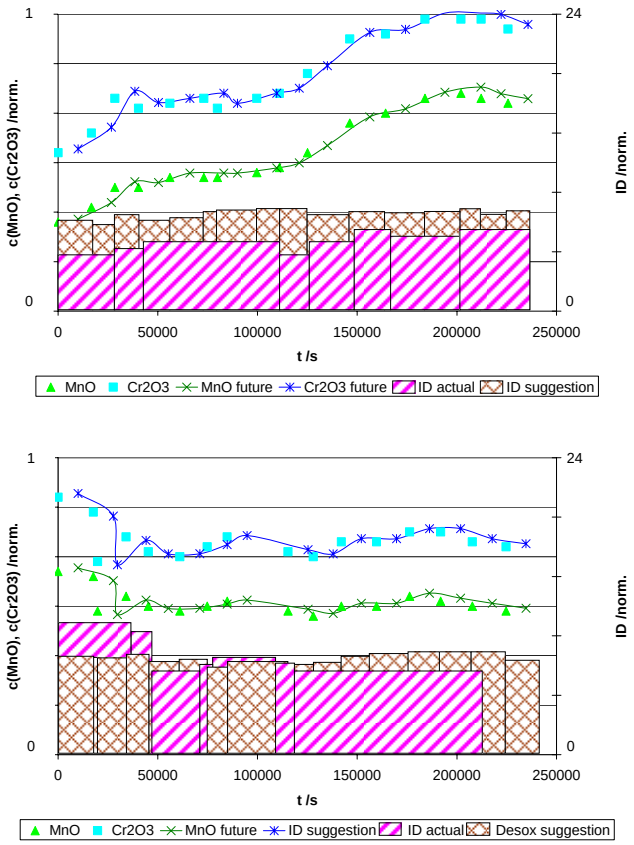

Figure 9: Actual evolution of oxide content in the slag over melting time and 10000s forecast based on the established model for two melts a, b

As explained in 3.9 the reverse function of the model, eq. (18), was applied to suggest a future ID for every stage in melting in order to simulate the on-line application of the model. The suggestion was calculated on an arbitrary preset for a fixed slagging rate SR. In a true industrial melt this rate will be adjusted, according to the actual metal concentration in the electrode and the desired metal concentration in the block, as can be derived from the mass balance established in 3.5. Results of the simulated application of the model can be compared to actual ID values in Figure 9 a, b.

5 Discussion and Conclusions

Conditions of slag sampling, chemical analysis and accurate data acquisition impose the first challenge on the model to be established. To examine the time dependency on kinetic effects, accurate recording of times for events like sampling or charging is crucial, yet not always easy to achieve. Several electrode changes during the melt and changes in their compositions impose further distortion to the system observed. All these factors cause the deviations that can be observed in the above plots. Yet, the model predicts the right tendencies in the behaviour of the system, the design of the predictions is robust and the process is dynamic in the sense that accuracy will improve with the acquisition of further melting data. The model is aimed to stabilize the process by enhanced control of desoxidation feed, i.e. the more stable the melts become, the more stable should be the database of the model as the set of conditions narrows down.

In a first approach 120 sets of melting data were analysed and a model was built upon, which correctly predicts the slag-metal reactions in local timeframes. This model has been inversely applied to suggest the necessary addition of desoxidation agents in order to achieve a desired rate of slagging. In the upcoming months this model will be transferred to set-up an expert system for improved process control and minimisation of fluctuations in ingot composition.

6 References

[1] G. Pateisky, H. Biele, H.J. Fleischer “The Reactions of Titanium and Silicon with Al_2O_3-CaO-CaF_2 Slags in the ESR Process”, J. Vac. Sci. Technol., Vol. 9, No. 6, 1972

[2] M. Etienne, A. Mitchell, “Oxidative Losses of Low Levels of Titanium During Electroslag Remelting”; Second International Symposium on Electroslag Remelting Technology, Pittsburgh 1969, Proceedings Part II

[3] Reitz, J.; Friedrich, B., “Fundamental of deoxidation behaviour of Ti-alloys by chamber ESR with Ca-reactive slags”; EMC 2007, June 11 - 14, Düsseldorf, Germany.

[4] D.R. Gaskell, „Structural Aspects of slags“; proceedings of the Molten Slags, Fluxes and Salts Conference, 1997, p. 11-26

[5] S. Seetharaman, L.I. Staffanson, “The solubility of Chromium ind Chromium(II) Chloride”, Acta Chemica Scandinavica A 30, 1976

[6] Jung-Ho, Park, Chang-Hee Rhee, „Ionic properties of oxygen in slag“; Journal of Non-Crystalline Solids“, Vol. 282, 2001, p. 7-14

[7] M. Sasabe, K.S. Goto; “Permeability, Diffusivity and Solubility of Oxygen Gas in Liquid Slag”; Metallurgical Transactions, Volume 5, October 1974, p. 2225-2233

[8] Hernandez-Morales, B., Mitchell, A., „Review of mathematical models of fluid flow, heat transfer and mass transfer in electroslag remelting process”; Ironmaking and Steelmaking Vol. 26 (1999) No. 6, p. 423-438

[9] G. Hoyle, “Electroslag processes – Principles and Practice”; Applied Science Publishers Ltd., 1983, ISBN: 0-85334-164-8